Formation Mechanism of Nanotubes in GaN

Z. Liliental-Weber, Y. Chen, S. Ruvimov, and J. Washburn
Lawrence Berkeley National Laboratory 62/203, Berkeley, California 94720
(Received 10 February 1997)

A formation mechanism for so-called nanotube defects in GaN is proposed. It is shown that two related types of defects are formed: nanotubes and pinholes. Both start with V shaped facets on $\{10\bar{1}1\}$ polar planes. Slow growth rate on these polar planes and impurity poisoning of growth steps are suggested as being responsible for initiation of these defects. [S0031-9007(97)04246-4]

PACS numbers: 61.72.Qq, 68.55.Ln, 78.55.Cr

Thin film epitaxy of polar materials grown by molecular beam epitaxy (MBE) is frequently associated with the formation of structural defects. One such defect is the so-called "microtube" observed in SiC, Al_2O_3, and ZnO [1–3]. These defects are empty hollows extending along the growth direction. Their size in SiC is in the range of a fraction of a micrometer to several micrometers, and their density is in the range of 100 to 1000 cm^{-2}. Recently, characteristic defects were found in epitaxially grown GaN, which are smaller in diameter than the microtubes in SiC and, therefore, have been called nanotubes [4,5]. They always extend along the c-axis growth direction of the film. Their density was estimated to be in the range of 10^5–10^7 cm^{-2}: They have radii in the range 3–1500 nm.

Frank [6] suggested that dislocations of large Burgers vector would have lower total line energy if the core was empty compared to a core filled with the highly strained lattice. According to Frank, the total energy is minimized when the empty core radius $r = \mu \mathbf{b}^2/8\pi^2\gamma$, where $\mathbf{b}$ is the Burgers vector of the dislocation, μ is the shear modulus, and γ is the specific surface energy. However, this model does not fit the experimental observations on GaN [4,7]. This Letter presents a possible formation mechanism of these nanotubes and related "pinhole" defects.

GaN samples grown by MBE and metal-organic chemical vapor deposition (MOCVD) on SiC, Al_2O_3, and on bulk GaN crystals were studied by plan view and cross-section transmission electron microscopy (TEM). The latter is critical to distinguish shallow indentations from defects that extend deeply into the layer. Both kinds of "holes" when studied in plan view have a perfect or slightly elongated hexagonal shape [Fig. 1(a)]. It is likely that some defects that have been assumed to be "nanotubes" do not have a substantial penetration along the growth direction and should not be called nanotubes. In general, this work shows that holes which have a hexagonal shape in plan view can be located at different depths in the layer: Some start only in the near surface area [Figs. 1(b) and 2(a) and defect A in Fig. 2(b)], some start and terminate within the layer [Figs. 1(c), 1(d), and 2(c)], and some start near the interface with the substrate and extend through the entire layer [defect B in Fig. 2(b)]. To distinguish between these different defects the ones that do not have a substantial length with a constant diameter extending along the growth direction will be called as pinholes [Fig. 1(b) and Figs. 2(a)–2(c)]. Only TEM studies in cross section can clearly distinguish between a pinhole and a nanotube.

The usual diameter of a nanotube in GaN is observed to be in the range of 2–40 nm, but pinholes can extend in diameter at the sample surface to a few hundred nanometers (300–800 nm). Both types of defects may

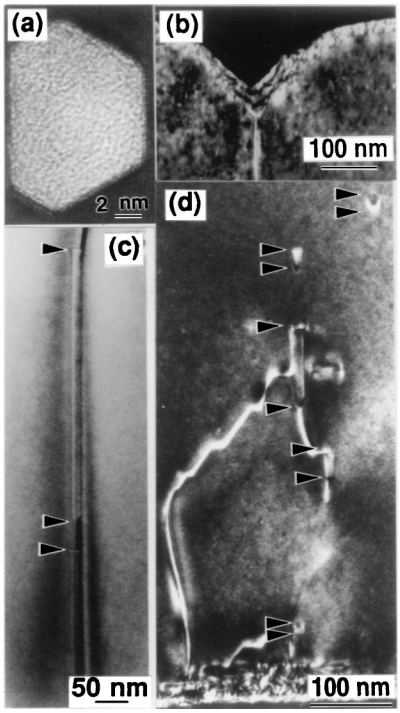

FIG. 1. (a) Plan-view TEM micrograph of a pinhole in a GaN sample grown by MOCVD on Al_2O_3. (b) Cross-section TEM micrograph showing a dislocation in a GaN rich in oxygen (with mixed type Burgers vector) attached to a pinhole. (c) Cross-section TEM micrograph showing two nanotubes along the growth direction aligned with a screw dislocation. This dislocation has been attracted to the tube. Note that the nanotube starts from a pinhole with V shape, and then changes to the tubular shape, and that nanotubes also terminate with overgrowth of perfect material on top. (d) Nanotubes formed above a buffer layer attached to the half-loop and nanotubes not related to dislocations (right-hand corner of the micrograph).

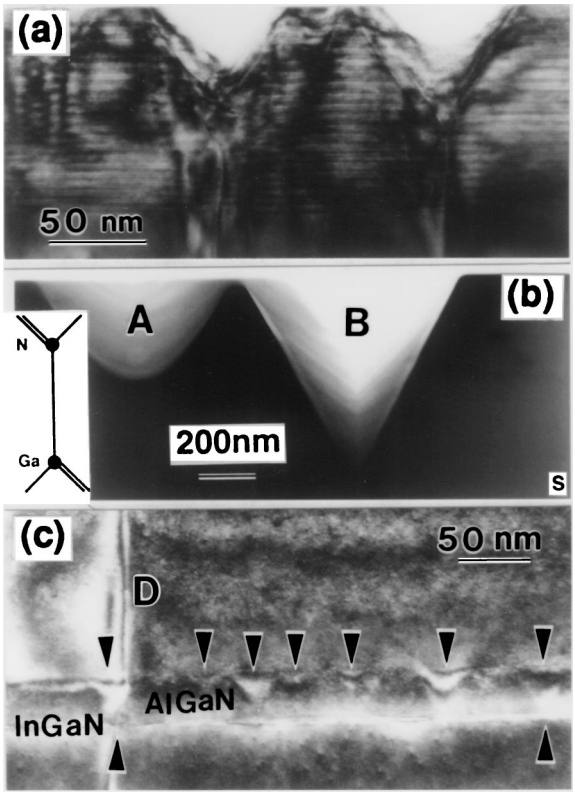

FIG. 2. (a) Pinholes formed at InGaN/GaN MQW's. (b) Pinholes formed in a homoepitaxial GaN layer grown on a bulk GaN substrate (S). Both defects were not related to any line or extended defect. Pinhole "A" was formed in the middle of the layer; pinhole "B" was formed close to the interface with the substrate. Polarity of the layer is indicated. (c) Pinholes formed at the InGaN layer (lower arrows) and AlGaN layers (upper arrows). Note that all of them were overgrown with a GaN on top of them. Only one dislocation (D) is shown on this micrograph. Note many pinholes formed in the dislocation free areas and presence of microinhomogeneities in the form of small dots.

have the same origin; nanotubes may develop from what was originally a pinhole. Both defects start with a characteristic V shape in cross section with about 60° between the V arms.

Many nanotubes were found to start above the buffer layer (80–1500 nm from the interface with a substrate) and were associated with dislocation half-loops formed in this area [Fig. 1(d)], but many also start at other locations within the layer. The majority of nanopipes ($\frac{2}{3}$) have an almost constant diameter (11 to 13 nm) but some were only 2–5 nm in diameter and others up to 30 or 40 nm in diameter. The diameter did not appear to be in sets with specific sizes. Their length along the c axis also varied between 10–400 nm [Figs. 1(c) and 1(d)]. Some nanotubes line up with others along straight threading dislocations [Fig. 1(c)], but others are attached to curving dislocations or are not connected with dislocations at all [Fig. 1(d), upper right corner].

No correlation was found between the overall density of dislocations and the density of nanotubes. For GaN crystals doped with Si (9×10^{16} to 1×10^{19} cm^{-3}) a decrease of dislocation density was observed from 1×10^{10} to 3×10^{9} cm^{-2} [5]. However, in the same samples the density of nanotubes increased markedly from 1×10^{6} to $6–8 \times 10^{7}$ cm^{-2}.

The near surface pinholes have the same V shape as the bottom of a nanotube but the sides of the V extend to the sample surface [Figs. 1(b) and 2(a) and 2(b)]. The number of pinholes increases dramatically with an increase in the concentration of certain impurities. In layers where oxygen content was increased from 5×10^{17} cm^{-3} to 4×10^{18} cm^{-3} the density of pinholes increased from 7×10^{6} cm^{-2} to 5×10^{7} cm^{-2}, and their diameter changed from 100 nm to 300–1500 nm [Fig. 1(b)]. The density of nanotubes also increased from 1×10^{7} to 3×10^{7} cm^{-2} without any measurable change of the dislocation density or lattice parameter.

Addition of dopants such as Mg, Al, or In also leads to increased formation of pinholes. For layers with In multiquantum wells (MQW) a dramatic change of pinhole density and their diameters was observed as the number of QW increased [Fig. 2(a)]. They originated randomly, starting usually with the second QW. For higher In concentration more pinholes are formed even when a single QW is grown. Their density dramatically increases when an AlGaN layer is grown on top of the In QW [Fig. 2(c)]. In a limited number of cases it was observed that pinholes were terminated by growth of oxygen free GaN. In most cases, however, once a pinhole is formed it extends to the surface along V arms.

Additional information about formation of these empty hollow defects was obtained by a study of homoepitaxial GaN layers grown on bulk GaN platelets. These epitaxial layers are essentially strain free but they adopt the substrate polarity and develop different types of defects and different surface morphology depending on this growth polarity [8]. Pinhole defects were found for homoepitaxial layers grown with both polarities. For layers grown in the polar direction Ga to N (defined here as A polarity) their density was high ($10^{6}–10^{7}$ cm^{-2}), while for growth in the opposite polarity the density was about 2 orders of magnitude smaller and most of them were associated with inversion domains. Pinholes observed for layers grown with A polarity were not related to any extended defects [Fig. 2(b)]. Growth on this side was so free of interfacial defects that it was impossible to determine the exact location of the original interface. If one assumes that the "deepest" pinholes [B in Fig. 2(b)] started at the substrate interface, then the thickness of the homoepitaxial layer would be 0.7 μm compared to the 1.2 μm layer thickness of the layer grown with B polarity. This is the first observation that growth with A polarity along the c direction is almost 2 times slower than growth with B polarity under identical growth conditions.

Initiation of the growth on the smooth side [B polarity—Fig. 3(a)] appeared to be more difficult. Dark field electron microscopy shows inhomogeneities at the

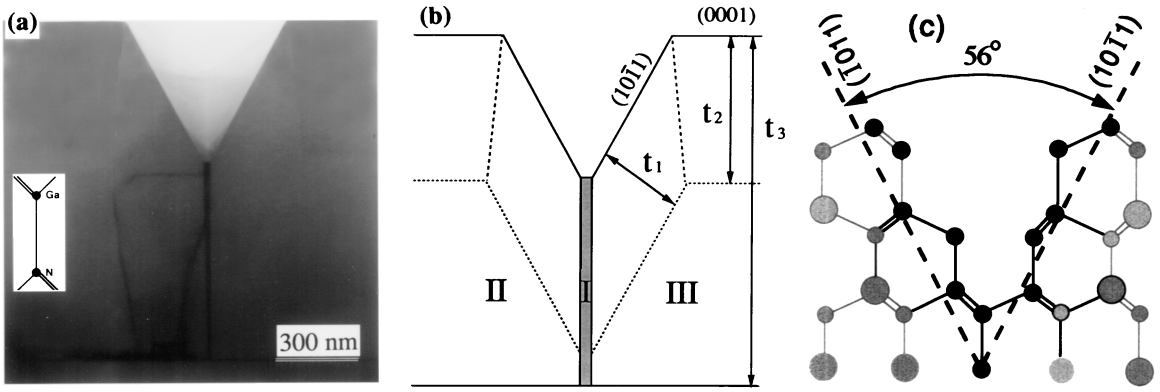

FIG. 3. (a) Cross section of a homoepitaxial GaN layer grown in *B* polarity on bulk GaN. Two dislocations and an inversion domain are associated with the pinhole. The height of the inversion domain (I) is about half the surrounding layer thickness t_3, showing different growth rates for the two polar directions. Two subgrains [marked in (b) as II and III] are growing on the two sides of the inversion domain. Growth proceeds on top of these grains with thickness t_2 along the *c* axis and t_1 perpendicular to the $(10\bar{1}1)$ planes. The above micrograph is shown schematically for better clarity in (b). (c) Atomic model of a GaN crystal in $[1\bar{2}10]$ projection showing the atom arrangement along polar $(10\bar{1}1)$ planes. Note the same angle between these faceted planes and the V arms of the pinhole. Black disks are showing how a pinhole might be started at an impurity (or dopant) cluster; however, the cluster size is not indicated.

interface in the form of foreign or native atom clusters, islands, or dislocation loops. Further growth on top of such loops often lead to nucleation of inversion domains. From careful observations of the contrast near the inversion domain [marked I on Fig. 3(b)] it appears that the growth started three dimensionally. Two islands of GaN apparently formed at the interface [marked II and III in the schematic drawings—Fig. 3(b)], on both sides of the inversion domain. As shown in Figs. 3(a) and 3(b) a pinhole eventually developed on top of the inversion domain. The growth of the inversion domain was much slower than the two surrounding islands. Measurements of the layer thickness ($t_3 \sim 1.2$ μm) and the height of the inversion domain (0.75 μm) show that the growth rates for the two opposite polarities had a ratio of about 2 to 1 in agreement with the previous estimate.

From the contrast difference within the islands [II and III on Fig. 3(b)] and above them, on the two sides of the inversion domain [Fig. 3(a)], it appears that the growth of the islands proceeded in two directions: along the *c* axis at the top and on faceted walls of the islands inclined to the *c* axis. These faceted island walls were parallel to low energy $(10\bar{1}1)$ polar planes. By measuring the layer thickness t_2 on the top of the islands along the *c* axis and on the sides of the $(10\bar{1}1)$ facets t_1, it can be estimated that the growth rate on these polar planes was 2 to 2.5 times slower in comparison to the growth in the *c* direction. Dependence of growth rate on a growth direction is also clearly demonstrated by the shape of bulk GaN platelets. Based on measurement of typical GaN plate dimensions growth in the nonpolar directions $[1\bar{1}00]$ and $[1\bar{2}10]$ is up to 50–100 times faster than in the polar *c* direction [8].

The growth on $(10\bar{1}1)$ planes is the slowest, and also not equal, for *A* and *B* polarity. This suggests that whenever a facet is formed on these slowest growth planes this can originate a pinhole. This study of homoepitaxial films as well as earlier studies of heteroepitaxial GaN films [9] shows that islands which are formed at the origin of growth are always faceted on $(10\bar{1}1)$ polar planes. These facets are inclined about 30° to the *c* axis. A V shape with an angle of about 60° forming where neighboring islands with these polar facets meet. This is in agreement with all the experimental observations that both pinholes and nanotubes start with a V-shaped feature of about 60° between the arms and agrees with the angle between two $(10\bar{1}1)$ planes; the calculated angle between two polar $\{10\bar{1}1\}$ planes is 56.1°.

Since heteroepitaxial layers of GaN always have a high density of dislocations, it is difficult to determine if these dislocations are always associated with nucleation of these "hollow" defects or if they are attracted to these holes later so as to reduce line energy. No adequate model explaining all the experimental observations has been proposed for GaN up to the present [4,5,7]. The Frank equilibrium model cannot explain the presence of these empty hollow defects, since the experimentally measured Burgers vectors typically associated with such defects is about 1 order of magnitude smaller than the Burgers vector calculated from Frank's equation [6]. Figure 3(a) shows two dislocations attracted to the inversion domain and then to the pinhole. It can be seen that the inversion domain and the dislocations were independently formed at the interface. As growth proceeded the dislocation eventually intersected the facet of the pinhole. During further growth the dislocations then propagated toward the hole in order to minimize their length and, therefore, minimize the total free energy of the system. Diffraction contrast showed that these two dislocations were of different Burgers vector, the lower dislocation closer to the inversion domain initially had a near screw character,

while the upper one was lying at a larger angle to its Burgers vector. This example shows that dislocations that are often attached to these pinholes observed in plan-view studies are not necessarily involved with the pinhole formation. They can be attracted to pinholes or nanotubes to decrease total line energy, but may not always be involved in the nucleation. Formation of facets on the slow growth $\{10\bar{1}1\}$ planes appears to be the critical event leading to pinhole nucleation. Any development of surface roughness during growth such as at places where growth islands meet each other, where a dislocation intersects the growth surface, impurity clusters, are all potential places where pinholes can originate due to the slow growth rate on $(10\bar{1}1)$ facets. Figure 3(c) shows an atomic model of a pinhole at an early stage as it might develop due to segregation of impurities to an indentation.

Our observations show that growth instabilities, increase of local strain due to introduction of dopant, or impurities such as oxygen appear to increase formation of these defects. In Mg-doped samples grown on Al_2O_3 the density of nanotubes was in the range of 7×10^7 cm^{-2} compared to 1×10^6 cm^{-2} in undoped GaN samples grown on the same substrate. In Si doped samples with an increase of dopant concentration the concentration of pinholes also increases. A similar observation of a higher density of pinhole formation was observed when In was added during the growth of quantum wells. These examples suggest that increase of strain in the layer is one factor that affects formation of pinholes. However, the formation of pinholes in strain free homoepitaxial layers [Figs. 2(b) and 3(a)] as well in the samples with increased oxygen [Fig. 1(b)] where no change of the lattice parameter was observed suggest that strain is not a necessary condition for formation of a pinhole. The experimental observations suggest that impurities or dopant elements play a role in the nucleation of pinholes and in the development of some into nanotubes.

The growth of nanotubes may be analogous to growth of whisker crystals where growth on the side surfaces is prevented by impurity poisoning of growth sites. Growth of a nanotube can be thought of as the mirror image of whisker crystal growth. As is the case for whisker growth, it is then not surprising that continued propagation of a nanotube appears to be very sensitive to growth conditions and change of impurity concentration. An impurity cluster may locally impede growth resulting in a small indentation that could be the nucleus of a pinhole. The evolution of some of these pinholes with $\{10\bar{1}1\}$ facets into long nanotubes requires that the $\{10\bar{1}1\}$ facets become $\{10\bar{1}0\}$ facets parallel to the growth direction. In an ideal clean environment such a nanotube would "recover" since growth on $\{10\bar{1}0\}$ planes should be rapid as was observed for bulk GaN platelets. However, impurity "poisoning" of the $\{10\bar{1}0\}$ facets could stabilize empty cylinder propagation in the same way that impurity poisoning stabilizes whisker growth in many materials. Termination of nanotubes might take place as shown on Figs. 1(c), 1(d), and 2(c), if the local impurity segregation falls below some critical level.

In conclusion, it has been suggested that the origin of nanotubes and pinholes in epitaxial polar materials may be related to growth kinetics on particular crystallographic planes, and impurity poisoning of growth steps. Two types of related defects (pinholes and nanotubes) have been identified in GaN samples. Formation of a nanotube appears to require nucleation of a pinhole. Pinhole formation results from slow growth rate on polar $(10\bar{1}1)$ planes resulting in the observed V shaped features, with about 60° between the arms, in good agreement with the angle between two $\{10\bar{1}1\}$ planes. Formation of nanotubes and large pinholes could possibly be eliminated by reduction of impurity levels below some critical value which would probably be dependent on growth rate and on choice of substrate orientation.

This work was supported by the U.S. Department of Energy under the Contract No. DE-AC03-76SF00098. The use of the facility at the National Center for Electron Microscopy at the LBNL is greatly appreciated. The authors want to thank Dr. J. Baranowski, Dr. H. Amano, Dr. I. Akasaki, Dr. S. Nakamura, Dr. Y. Yang, and Dr. W. Imler for providing the GaN samples, W. Swider for the excellent sample preparation and photographic work, and Dr. E. R. Weber and Dr. J. Ager for the suggestion to improve this manuscript.

[1] H. M. Hobgood, D. L. Barret, J. P. McHugh, R. C. Clarke, S. Sriram, A. A. Burk, J. Greggi, C. D. Brandt, R. H. Hopkins, and W. J. Choyke, J. Cryst. Growth **137**, 181 (1994).

[2] S. Takasu and S. Shimanuki, J. Cryst. Growth **24/25**, 641 (1974).

[3] J. Heindl and H. P. Strunk, Phys. Status Solidi (b) **193**, K1 (1996).

[4] W. Qian, G. S. Rohrer, M. Skowronski, K. Doverspike, L. B. Rowland, and D. K. Gaskill, Appl. Phys. Lett. **67**, 2284 (1995).

[5] Z. Liliental-Weber, S. Ruvimov, T. Suski, J. W. Ager III, W. Swider, J. Washburn, H. Amano, I. Akasaki, and W. Imler, Mater. Res. Soc. Symp. Proc. **423**, 487 (1996).

[6] F. C. Frank, Acta Crystallogr. **4**, 497 (1951).

[7] F. A. Ponce, D. Cherns, W. T. Young, J. W. Steeds, and S. Nakamura, Mater. Res. Soc. Symp. Proc. **449**, 405 (1997).

[8] Zuzanna Liliental-Weber, C. Kisielowski, S. Ruvimov, Y. Chen, J. Washburn, I. Grzegory, M. Bockowski, J. Jun, and S. Porowski, J. Electron. Mater. **25**, 1545 (1996).

[9] X. H. Wu, P. Fini, S. Keller, E. J. Tarsa, B. Heying, U. K. Mishra, S. P. DenBaars, and J. S. Speck, Jpn. J. Appl. Phys. **35**, L1648 (1996).